Dear Deuta and Maa

“For your love - steady as the stars,

For your strength - quiet, constant,

For every unseen sacrifice,

Your heart and hustle built me,

This thesis is my ‘Thank you’.”

Dedicated to my parents Mr. Ashyut Baishya and

Mrs. Ibharani Baishya.

Declaration by the Candidate

I hereby declare that the thesis "***Investigation on Electroactive Materials for Monovalent and Multivalent Ion-Based Energy Storage Devices***" being submitted to the Department of Physics, Tezpur University under the School of Sciences in partial fulfillment for the award of the degree of Doctor of Philosophy in Physics. This is an original work carried out by me and it has not been previously considered for the award of any degree, diploma, associateship, fellowship or and other similar title or recognition from any University, Institute or other organization.

Ritupurna Baishya

(Ritupurna Baishya)

Regd no.: TZ155652 of 2015

Date: 06-08-2025

Place: Tezpur, Assam

तेजपुर विश्वविद्यालय/ **TEZPUR UNIVERSITY**
(संसद के अधिनियम द्वारा स्थापित केंद्रीय विश्वविद्यालय)
(A Central University established by an Act of Parliament)
तेजपुर-784028 :: असम/ **TEZPUR-784028 :: ASSAM**

(सर्वोत्तम विश्वविद्यालय के लिए कुलाध्यक्ष पुरस्कार,2016 औरभारत के 100श्रेष्ठ उच्च शिक्षण संस्थानों में पंचम स्थान प्राप्त विश्वविद्यालय)
(Awardee of Visitor's Best University Award, 2016 and 5th among India's Top 100 Universities, MHRD-NIRF Ranking, 2016)

Dr. Shyamal Kumar Das skdas@tezu.ernet.in
Assistant Professor
Department of Physics
School of Sciences

Certificate of the Supervisor

This is to certify that the thesis entitled ***"Investigation on Electroactive Materials for Monovalent and Multivalent Ion-Based Energy Storage Devices"*** submitted to the School of Sciences, Tezpur University in partial fulfillment for the award of the degree of Doctor of Philosophy in **Department of Physics** is a record of original research work carried out by **Mr. Ritupurna Baishya** under my personal supervision and guidance.

All helps received by him from various sources have been duly acknowledged.

No part of this thesis has been reproduced elsewhere for award of any other degree.

Shyamal Kr Das

Date: 06.08.2025 (Dr. Shyamal Kumar Das)

Place: Tezpur University

तेजपुर विश्वविद्यालय/ **TEZPUR UNIVERSITY**
(संसद के अधिनियम द्वारा स्थापित केंद्रीय विश्वविद्यालय)
(A Central University established by an Act of Parliament)
तेजपुर-784028 :: असम/ **TEZPUR-784028 :: ASSAM**

(सर्वोत्तम विश्वविद्यालय के लिए कुलाध्यक्ष पुरस्कार,2016 औरभारत के 100श्रेष्ठ उच्च शिक्षण संस्थानों में पंचम स्थान प्राप्त विश्वविद्यालय)
(Awardee of Visitor's Best University Award, 2016 and 5th among India's Top 100 Universities, MHRD-NIRF Ranking, 2016)

Certificate of the External Examiner and ODEC

This is to certify that the thesis entitled "***Investigation on Electroactive Materials for Monovalent and Multivalent Ion-Based Energy Storage Devices***" submitted by **Mr. Ritupurna Baishya** to Tezpur University in the **Department of Physics** under the School of Sciences in partial fulfillment of the requirement for the award of the degree of Doctor of Philosophy in Physics has been examined by us and found to be satisfactory.

The Committee recommends for the award of the degree of Doctor of Philosophy.

.

Principal Supervisor
Date:

External Examiner
Date:

Acknowledgement

Firstly, I would like to express my heartfelt gratitude to my honored supervisor ***Dr. Shyamal Kumar Das****, whose excepted brilliance, infectious enthusiasm, and unwavering discipline have profoundly shaped my PhD journey. Your remarkable ability to distil complex ideas into clear, actionable insight has been a constant source of inspiration for me. I am profoundly grateful for his generosity, patience, and belief in my potential. You have not only shared your vast knowledge but also created an environment where I felt empowered to experiment, learn from mistakes and celebrate achievements. Your mentorship has been a transformative force, and I am truly honored to have had the opportunity to learn from someone like you. Thank you for everything.*

I would also like to extend my gratitude towards ***Dr. S. R. Barman****, Scientist-H, UGC-DAE CSR, Indore for the project support and his constant guidance.*

I want to convey my sincere gratitude to my doctoral committee members ***Prof. Dambarudhar Mohanta*** *and* ***Dr. Rajib Biswas*** *for their support and encouragement during my PhD tenure.*

I want to express my gratitude to former Vice Chancellors, ***Late Prof. M. K. Choudhury****,* ***Prof. V. K Jain*** *and current Vice Chancellor* ***Prof. Shambhu Nath Singh*** *of Tezpur University, for providing all the facilities needed on the university campus to conduct my research.*

I am really grateful to ***Prof. Pabitra Nath****, Head of the Physics Department, former Head of the Physics Department* ***Prof. Mrinal Kumar Das****, for all the kind assistance and support throughout my PhD journey in the Department. I am also thankful to the entire faculty members of the Department of Physics for their helpful assistance and support during my PhD tenure.*

I would also like to thank the ***Dean, School of Sciences****, Tezpur University for the academic support and generosity.*

I would like to thank ***Prof. Manabendra Mandal****, Dean of Student Welfare and* ***Mr. Kumarjit Dutta,*** *Deputy Registrar, Finance for their constant support and guidance.*

I am always thankful to the technical and non-technical staff members of Department of Physics and SAIC, Tezpur University: ***Dr. Kishore Baruah****,* ***Dr. Ratan Baruah, Mr. Narayan Sharma, Mr. Palash Dutta, Mr. Biju Boro, Mr. Mrinmoy Gohain, Mr.***

Prakash Kurmi, Mr. Tridib Ranjan Nath, Mr. Nava Kr. Gogoi, Mr. Dhruba Deka, Mr. Umesh Patir and Mr. Suman Sarmah *for their help.*

I want to sincerely thank ***Dr. Hridoyjit Phukan****, NEIST, Jorhat, for all the help with my research objectives.*

Many thanks to my lab mates- ***Dr. Homen Lahan, Dr. Devalina Sarmah, Dr. Sunny Nandi, Dr. Atowar Rahman, Ms. Konica Roy, Ms. Padmini Priyanka and Mr. Bali Kamum*** *for helping me with their suggestions and fruitful discussions.*

I would also like to thank my friends ***Ashok, Rajon, Nandit and Pranjit*** *for all-time support and encouragement. I am indeed lucky to have some lively juniors,* ***Kaushik, Hritwik, Niranjan, Dhanjit, Jubaraj, Anil****,* ***Debashish*** *and* ***Biplob****. I would like to thank some of my friends and seniors,* ***Nikhil Da****,* ***Upama, Bhabana, Arnab, Jotin Da, Prankrishna Da, Lavina Ba, Sritam Da, Hirak Da and Debabrata Da*** *for the all the help and support. I would also like to thank all the members of department of Physics for their encouragement during this period of my life*

I would like to thank ***Ankita Kakoti*** *for being there with me in every ups and down and giving constant moral support throughout this journey.*

Hereby, I take the opportunity to thank my greatest source of motivation, ***Deuta*** *and* ***Maa*** *for their boundless love and encouragement. Your nurturing presence have always been my anchor, providing me with the strength to navigate challenges and the courage to chase my dreams. The weight of your influence humbles me and the warmth of your pride fuels my determination to honor you with my choices. Thank you from core of my being, for being my parents, my heroes, and my home.*

I thank all those people who helped me in many other ways yet whose name couldn't be mentioned.

At last, I thank almighty for keeping me safe, happy, and going forward.

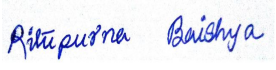

-Ritupurna Baishya

Acknowledgement to UGC, DAE CSR

The thesis work was partially carried out using the facilities of UGC-DAE CSR. We acknowledge the financial support from UGC-DAE CSR through a Collaborative Research Scheme (CRS) project number **CRS/2021-22/01/354**.

Ritupurna Baishya

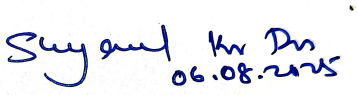

Dr. Shyamal Kumar Das

List of Tables

Table No.	Table caption	Page No.
	CHAPTER 3:	
	The Active-Inactive Interface for K^+ Ion Storage- A Case Study with $Bi_5Nb_3O_{15}$	
Table 3.1.	R1, R2, R3, R4 values of $Bi_5Nb_3O_{15}$ from the fitted EIS data of figure 3.8 (a-c) in different substrates in aqueous 3 M aqueous KOH electrolyte.	66
Table 3.2	Time dependent R_1, R_2, R_3, R_4 values of bare substrates from the fitted EIS data of figure 3.9. Electrolytes used here is aqueous 3M aqueous KOH electrolyte.	68
Table 3.3	Contact angle values of $Bi_5Nb_3O_{15}$ for different substrates after before, 1^{st} and 100^{th} discharge state electrode.	69
Table 3.4	Overpotential of $Bi_5Nb_3O_{15}$ after 1^{st} and 2^{nd} discharge. D: discharge, C: charge.	70
Table 3.5	Contact angle values of different substrates without $Bi_5Nb_3O_{15}$ before and after dipping in KOH electrolyte.	70
Table 3.6	Different parameters obtained from extrapolation of tafel plot.	74
	CHAPTER 4:	
	Investigation on Al^{3+} ion storage in Bi_2MoO_6 and Bi_2WO_6 for rechargeable aqueous aluminum-ion battery	
Table 4.1	Charge transfer resistance values obtained from fitting the EIS data shown in previous figure	90
Table 4.2	Obtained band gap values. of Bi_2WO_6 before and after 1^{st} discharge, 1^{st} charge and 15^{th} discharge state, respectively.	97

CHAPTER 5:

High-rate performance of H_xMoO_3 for aqueous aluminium-ion battery

Table 5.1	Details of the characteristic Raman peaks observed in MoO_3	107
Table 5.2	Peak to peak separation from Cyclic Voltammetry	111
Table 5.3	Specific Capacities after discharge and charge of MoO_3 and H_xMoO_3 at different current densities	114
Table 5.4	Peak separation from GCD of MoO_3 and H_xMoO_3 at different current densities	116
Table 5.5	Charge transfer resistance (R_3) values from EIS fitting.	121

List of Figures

Figure No.	Figure caption	Page No.
	CHAPTER 1:	
	Introduction	
Figure 1.1	Schematic of current global energy usage.	1
Figure 1.2	Schematic of current global energy infrastructure.	3
Figure 1.3	Schematic of battery-based storage utilities.	5
Figure 1.4	Schematic representation of an aqueous battery.	10
	CHAPTER 2:	
	Aqueous electrolyte mediated reversible K^+ ion insertion in graphite	
Figure 2.1.	(a) XRD patterns, (b) Raman spectra and (c,d) FESEM images of Natural and Pyrolytic graphite.	38
Figure 2.2	CV profiles of Natural graphite in aqueous (a) 1M KOH, (b) 6M KOH, CV profiles of (c) Exfoliated graphite and (d) Pyrolytic graphite in 6 M aqueous KOH at a scan rate of 2.5 mVs^{-1}.	39
Figure 2.3	Galvanostatic discharge/charge profiles of (a) 200 mAg-1, (b) 400 mAg^{-1}, (c) 2000 mAg^{-1} and (d) rate capability measurement of Natural graphite in 1 M KOH aqueous electrolyte.	39
Figure 2.4	Galvanostatic discharge/charge profiles of (a) 200 mAg^{-1}, (b) 400 mAg^{-1}, (c) 2000 mAg^{-1} and (d) rate capability measurement of Natural graphite in 6 M KOH aqueous electrolyte.	40
Figure 2.5	Galvanostatic discharge/charge profiles of (a) 200 mAg^{-1}, (b) 400 mAg^{-1}, (c) 2000 mAg^{-1} and (d) rate capability measurement of exfoliated graphite in 6 M KOH aqueous electrolyte.	41
Figure 2.6	Galvanostatic discharge/charge profiles of (a) 200 mAg^{-1}, (b) 400 mAg^{-1}, (c) 2000 mAg^{-1} and (d) rate capability measurement of exfoliated graphite in 1 M KOH aqueous electrolyte.	42
Figure 2.7	Comparison of Rate capability measurement of normal and exfoliated graphite in 6 M KOH aqueous electrolyte.	42
Figure 2.8	Charge/discharge curve of pyrolytic graphite in 6 M KOH electrolyte at 200 mAg^{-1}.	43

Figure 2.9	(a) CV curves of natural graphite at different scan rates and (b) plot of peak current vs scan rate. (c) Capacitive and diffusive contributions for 6 M KOH in natural graphite at 2.5 mVs^{-1}, (d) Log (peak current) vs Log (Scan rate), (e) Diffusive and capacitive contributions in percentage. The electrolyte is 6 M KOH.	44
Figure 2.10	(a-b) Ex-situ XRD analysis, (c-d) Raman spectra of pristine graphite, natural graphite after 1^{st} and 50^{th} Discharge.	45
Figure 2.11	High resolution XPS spectra for (a) Full XPS spectrum (b) C 1s, (c) O 1s peaks, (d) O1s.	46
Figure 2.12	High resolution XPS spectra (after dipping natural graphite in KOH) for (a) Full XPS spectra, (b) C1s peak (no K2p peaks), (c) Enlarged C1s, (d) O1s.	46
Figure 2.13	AFM images of natural graphite (a,c) before discharge, (b,d) after discharge and (a, b) FESEM image of natural graphite after discharge.	47
Figure 2.14	(a-c) Contact angle measurement for natural graphite, EIS spectra for (d) natural graphite and pyrolytic graphite, (e) The relationship curve between Z' and $\omega^{-1/2}$ in the low-frequency range for natural graphite in 6 M KOH.	49

CHAPTER 3:

The Active-Inactive Interface for K^+ Ion Storage- A Case Study with $Bi_5Nb_3O_{15}$

Figure 3.1	a) XRD pattern and crystal structure of $Bi_5Nb_3O_{15}$ (Obtained from VESTA Ver. 3.90.1a), b) FESEM image, XPS spectra of c) Bi 4f and d) Nb 3d in $Bi_5Nb_3O_{15}$ b) FTIR spectrum of $Bi_5Nb_3O_{15}$.	58
Figure 3.2	a) XRD pattern and crystal structure of $Bi_5Nb_3O_{15}$ (Obtained from VESTA Ver. 3.90.1a), b) FESEM image, XPS spectra of c) Bi 4f and d) Nb 3d in $Bi_5Nb_3O_{15}$ b) FTIR spectrum of $Bi_5Nb_3O_{15}$..	59
Figure 3.3	Cyclic Voltammetry profile in aqueous a) K_2SO_4 b) KCl electrolyte at a scan rate of 2.5 mVs^{-1}, Galvanostatic charge	60

	discharge profiles in electrolyte in aqueous c) K_2SO_4 d) KCl electrolyte; Rate capability in aqueous e) K_2SO_4 f) KCl at current densities of 2 Ag^{-1} of $Bi_5Nb_3O_{15}$.The substrate used here is Titanium. (D: discharge, C: Charge)	
Figure 3.4	(a) Cyclic voltammetry profile at a scan rate of 2.5 mVs^{-1}, Galvanostatic charge discharge profiles at a current density of (b) 2 Ag^{-1}, (c) 5 Ag^{-1}, Rate capability at a current density of d) 1 Ag^{-1} d) 2 Ag^{-1} d) 5 Ag^{-1} of $Bi_5Nb_3O_{15}$ in 3M aqueous KOH electrolyte. The substrate used here is Stainless steel. (D: discharge, C: Charge)	61
Figure 3.5	a) Cyclic voltammetry profile at a scan rate of 2.5 mVs^{-1}, Galvanostatic charge discharge profiles of $Bi_5Nb_3O_{15}$ at b) 1 Ag^{-1}, c) 2 Ag^{-1} in 3M aqueous KOH electrolyte. The substrate used here is Nickel.	62
Figure 3.6	Cyclic voltammetry profile at a scan rate of 2.5 mVs^{-1}, Galvanostatic charge/discharge profiles at a current density of (b) 1 Ag^{-1}, (c) 5 Ag^{-1}, Rate capability at a current density of d) 1 Ag^{-1} d) 2 Ag^{-1} e) 5 Ag^{-1} of $Bi_5Nb_3O_{15}$. Electrolyte used here is 3 M aqueous KOH electrolyte. The substrate used here is graphite. (D: discharge, C: Charge).	63
Figure 3.7	Cyclic Voltammetry profile in aqueous a) K_2SO_4 and b) KCl electrolyte, Galvanostatic charge discharge profiles in electrolyte in aqueous c) K_2SO_4 and d) KCl electrolyte; Rate capability in aqueous e) K_2SO_4 and f) KCl at current densities of 2 Ag^{-1} of $Bi_5Nb_3O_{15}$.The substrate used here is graphite. (D: discharge, C: Charge).	64
Figure 3.8	Nyquist plots of $Bi_5Nb_3O_{15}$ after 1st D and 100th D on a) graphite, b) titanium; (c) Stainless Steel, bode plot of $Bi_5Nb_3O_{15}$ after (d) 1st D, (e) 100th D on different substrates and f) Fitting parameters. (D: discharge, C: charge).	65
Figure 3.9	Nyquist plots of $Bi_5Nb_3O_{15}$ after 1st D and 100th D on a) graphite, b) titanium; (c) Stainless Steel, bode plot of	67

	$Bi_5Nb_3O_{15}$ after (d) 1st D, (e) 100^{th} D on different substrates and f) Fitting parameters. (D: discharge, C: charge).	
Figure 3.10	Change in contact angle values of $Bi_5Nb_3O_{15}$ before and after 1^{st}, 100^{th} discharge state electrode in graphite, titanium, and Stainless-steel substrate.	69
Figure 3.11	Contact angle values for bare graphite, titanium, Stainless Steel, Nickel substrates without $Bi_5Nb_3O_{15}$ before and after dipping. (repeated two times).	70
Figure 3.12	FESEM images of bare Graphite, Titanium, Stainless Steel before and after dipping in KOH electrolyte.	72
Figure 3.13	Corrosion potential for (a) graphite, (b) titanium, (c) Stainless Steel, (d) Nickel substrates e) Fitted Tafel extrapolation Plots of different current collectors b) Comparison of corrosion rates and polarization resistances (R_p) calculated by fitting in the EC lab software.	73
Figure 3.14	**(**a-c) Ex-situ XRD analysis before and after 1^{st} D, 1^{st} C, and 100th D state electrodes, Ex-situ FESEM images after d) 1st D, and e) 100^{th} D state electrode. (D: discharge, C: charge)	75
Figure 3.15	(a,b) FTIR analysis of before and after discharged state electrodes (D:discharge, C: charge)	75
Figure 3.16	Ex-situ XPS spectra of (a) Full spectra, (b)K2p, (c) Bi4f, (d) Nb3d and (e) O1s in discharged state electrode of Bi5Nb3O15. (D: discharge, C: charge)	76

CHAPTER 4:

Investigation on Al^{3+} ion storage in Bi_2MoO_6 and Bi_2WO_6 for rechargeable aqueous aluminum-ion battery

Figure 4.1	XRD patterns (a) Bi_2MoO_6 and (b) Bi_2WO_6, FESEM image of (c) Bi_2MoO_6 and (d) Bi_2WO_6.	83
Figure 4.2	CV profiles of Bi_2MoO_6 (a) 1 M $AlCl_3$, (b) 0.5 M $AlCl_3$, (c) 0.5 M $Al_2(SO_4)_3$ aqueous electrolyte at a scan rate of 2.5 mVs^{-1}.	84
Figure 4.3	Galvanostatic charge discharge profiles of Bi_2MoO_6 in 1 M $AlCl_3$ at a current density of (a) 0.5 Ag^{-1}, (b) 1 Ag^{-1} and c) 2.5	85

	Ag^{-1}; c) Rate capability of Bi_2MoO_6 at different current densities in 1 M aqueous $AlCl_3$ electrolyte.	
Figure 4.4	Galvanostatic charge discharge profiles of Bi_2MoO_6 at a current density of (a) 0.5 Ag^{-1}, (b) 1 Ag^{-1} and c) 2.5 Ag^{-1}; c) Rate capability of Bi_2MoO_6 at different current densities in 0.5 M aqueous $AlCl_3$ electrolyte.	85
Figure 4.5	Galvanostatic charge discharge profiles of Bi_2MoO_6 at a current density of (a) 0.5 Ag^{-1}, (b) 1 Ag^{-1} and c) 2.5 Ag^{-1}; c) Rate capability of Bi_2MoO_6 at different current densities in 0.25 M aqueous $AlCl_3$ electrolyte.	86
Figure 4.6	Galvanostatic charge discharge profiles of Bi_2MoO_6 at a current density of (a) 0.5 Ag^{-1}, (b) 1 Ag^{-1} and c) 2.5 Ag^{-1}; d) Rate capability of Bi_2MoO_6 at different current densities in 0.5 M $Al_2(SO_4)_3$ aqueous electrolyte.	86
Figure 4.7	CV profile, Galvanostatic charge discharge profiles of Bi_2WO_6 at a current density of (b) 0.5 Ag^{-1} and (c) 2.5 Ag^{-1}; (d) Rate capability of Bi_2WO_6 at different current densities in 1 M aqueous $AlCl_3$ electrolyte.	87
Figure 4.8	Galvanostatic charge discharge profiles of Bi_2WO_6 at a current density of (a) 0.5 Ag^{-1}, (b) 1 Ag^{-1} and c) 2.5 Ag^{-1}; c) Rate capability of Bi_2MoO_6 at different current densities in 0.5 M aqueous $Al_2(SO_4)_3$ electrolyte.	88
Figure 4.9	Galvanostatic charge discharge profiles of Bi_2WO_6 at a current density of (a) 0.5 Ag^{-1}, (b) 1 Ag^{-1} and c) 2.5 Ag^{-1}; c) Rate capability of Bi_2WO_6 at different current densities in 1 M aqueous $AlCl_3$ electrolyte.	89
Figure 4.10	Galvanostatic charge discharge profiles of Bi_2WO_6 at a current density of (a) 0.5 Ag^{-1}, (b) 1 Ag^{-1} and c) 2.5 Ag^{-1}; (c) Rate capability of Bi_2WO_6 at different current densities in 1 M aqueous $AlCl_3$ electrolyte.	89
Figure 4.11	(a) EIS spectra of Bi_2WO_6 coated on Normal and exfoliated graphite in 0.5 M $AlCl_3$.	90

Figure 4.12	SEM images of (a-b) Normal graphite, (c-d) Exfoliated graphite, contact angle measurements of (c) Normal graphite, (f) Exfoliated graphite.	91
Figure 4.13	CV profile of Bi_2MoO_6 at different scan rate in a) 1 M $AlCl_3$ and b) 0.5 M $AlCl_3$. CV profile of Bi_2WO_6 at different scan rate in a)1 M $AlCl_3$ and b) 0.5 M $AlCl_3$	92
Figure 4.14	Ex-situ FESEM images of Bi_2WO_6 after (a-c) 1st discharge, (d-f) 1st charge, (g,h) HRTEM images, (i) SAED patterns of Bi_2WO_6, after 1st discharge.	92
Figure 4.15	Ex-situ XRD patterns of Bi_2WO_6 before and after 1st discharge, 1st charge and 15th discharge state, respectively.	93
Figure 4.16	High score plus analysis of BiOCl. Bi_2O_3, Al_2O_3 after discharged state electrode.	93
Figure 4.17	Ex-situ XPS spectra of (a) Bi4f and (b) W4f, (c) O1s, (d) Cl2p, (e) Al2p of Bi_2WO_6 before and after 1st discharge, 1st charge and 15th discharge state, respectively.	96
Figure 4.18	(a) Raman spectra, (g) FTIR spectra of Bi_2WO_6 before and after 1st discharge, 1st charge and 15th discharge state, respectively.	96
Figure 4.19	(a) UV-visible spectra before and after cycling, Tauc plots (b) before cycling, (c) After 1^{st} discharge, (d) after 1^{st} charge, (e) after 15^{th} discharge of Bi_2WO_6.	97

CHAPTER 5:

High-rate performance of H_xMoO_3 for aqueous aluminium-ion battery

Figure 5.1	(a-c) XRD analysis, (d) Raman spectra. (e) FTIR spectra of MoO_3 and H_xMoO_3.	106
Figure 5.2	FESEM images of (a,b) MoO_3 and (c,d) H_xMoO_3.	108
Figure 5.3	TEM images of (a) MoO_3 and (b) H_xMoO_3, HRTEM images, SAED patterns (left inset) and interlayer spacing after processing (right inset) of (c) MoO_3 and (d) H_xMoO_3.	108
Figure 5.4	a) Full XPS spectra, XPS spectra of b) Mo3d and c) O1s of MoO_3 and H_xMoO_3.	109

Figure 5.5	UV visible spectra of a) MoO_3, b) H_xMoO_3, c) Tauc plot obtained from the UV visible data d) PL spectra of MoO_3 and H_xMoO_3.	109
Figure 5.6	Multi-cycle CV curve of (a) MoO_3 and (b) H_xMoO_3, (c) Superimposition of the CV scan of MoO_3 and H_xMoO_3 in aqueous $AlCl_3$ electrolyte at a scan rate of 2.5 mVs^{-1}.	111
Figure 5.7	CV profile of a) MoO_3 and b) H_xMoO_3, c) Superimposition of the CV scan of MoO_3 and H_xMoO_3 in $Al_2(SO_4)_3$ aqueous electrolyte at a scan rate of 2.5 mVs^{-1}.	112
Figure 5.8	Galvanostatic charge discharge measurements of MoO_3 at current density of (a) 2 Ag^{-1}, (b) 5 Ag^{-1}, (c) 10 Ag^{-1}, (d) 20 Ag^{-1} in 1 M aqueous $AlCl_3$ electrolyte.	113
Figure 5.9	Galvanostatic charge discharge measurements of H_xMoO_3 at current density of (a) 2 Ag^{-1}, (b) 5 Ag^{-1}, (c) 10 Ag^{-1}, (d) 20 Ag^{-1} in 1 M aqueous $AlCl_3$ electrolyte.	113
Figure 5.10	Rate performance of MoO_3 and H_xMoO_3 at current density of (a) 2 Ag^{-1}, (b) 5 Ag^{-1}, (c) 10 Ag^{-1}, (d) 20 Ag^{-1} in 1 M aqueous AlCl3 electrolyte.	114
Figure 5.11	Comparison of 2nd cycle of galvanostatic charge discharge measurements of MoO_3 and H_xMoO_3 at current density of a) 2 Ag^{-1}, b) 5 Ag^{-1}, c) 10 Ag^{-1} and d) 20 Ag^{-1} in 1 M aqueous $AlCl_3$ electrolyte	116
Figure 5.12	CV profile of H_xMoO_3 in 1 M H_2SO_4 aqueous electrolyte at different scan rates.	117
Figure 5.13	FESEM images of H_xMoO_3 after discharge.	117
Figure 5.14	Galvanostatic charge discharge measurements of MoO_3 at current density of a) 2 Ag^{-1}, b) 5 Ag^{-1}, c) 10 Ag^{-1} in 0.5 M aqueous $Al_2(SO_4)_3$ electrolyte	118
Figure 5.15	Galvanostatic charge discharge measurements of H_xMoO_3 at current density of a) 2 Ag^{-1}, b) 5 Ag^{-1}, c) 10 Ag^{-1} in 0.5 M aqueous $Al_2(SO_4)_3$ electrolyte.	118
Figure 5.16	Rate performance of MoO_3 at current density of a) 2 Ag^{-1}, b) 5 Ag^{-1}, c) 10 Ag^{-1} in 0.5 M aqueous $Al_2(SO_4)_3$ electrolyte	119

Figure 5.17	Rate performance of H_xMoO_3 at current density of a) 2 Ag^{-1}, b) 5 Ag^{-1}, c) 10 Ag^{-1} in 0.5 M aqueous $Al_2(SO_4)_3$ electrolyte.	119
Figure 5.18	a) CV profile of the constructed $LiMn_2O_4$// H_xMoO_3 cell at a scan rate of 2.5 mVs^{-1}. Galvanostatic charge discharge measurements at current density of b) 80 mAg^{-1}, c) 250 mAg^{-1}, Rate performance at d) 80 mAg^{-1}, e) 250 mAg^{-1} of the constructed $LiMn_2O_4$ // H_xMoO_3 in 1 M aqueous $AlCl_3$ electrolyte	120
Figure 5.19	EIS spectra of MoO_3 and H_xMoO_3 after a)1st D and b)100th D; Bode plot after c)1st D and d)100th D.	121
Figure 5.20	The relationship curve between Z' and $\omega^{-1/2}$ in the low-frequency region.	122
Figure 5.21	GITT profile of (a) MoO_3, (b) H_xMoO_3, during one complete charge/ discharge cycle at a current rate 0.1 $mAcm^{-2}$ (c) Demonstration of a Single titration step during discharged state of H_xMoO_3 (d) enlarged view of one portion of the discharge curve with measured titration step highlighted on it; (e) GITT measurement of MoO_3 for one complete cycle, d) demonstration of a Single titration step during discharged state of MoO_3.	123
Figure 5.22	(a) XRD patterns of H_xMoO_3 after cycling, Enlarged view of the XRD patterns in the range of (b) 10^o -35^o, (c) 11^o -13^o (d) 20^o -30^o and (e) 33^o -35^o of discharged state electrode	124
Figure 5.23	(a-c) HRTEM and SAED pattern of discharged state electrode of H_xMoO_3 (D- discharge, C-charge).	125

LIST OF ABBREVIATIONS AND SYMBOLS

Abbreviation/Symbol		Name
%	:	Percent
LIB	:	Lithium-ion battery
AIB	:	Aluminum ion battery
Al	:	Aluminum
Al^{3+} ion	:	Aluminum ion
K^{+} ion	:	Potassium ion
Ca	:	Calcium
cm	:	Centimetre
Cu	:	Copper
Conc.	:	Concentration
mg	:	Milligram
Li	:	Lithium
Na	:	Sodium
K	:	Potassium
Zn	:	Zinc
Mg	:	Magnesium
Ca	:	Calcium
CV	:	Cyclic voltammetry
γ	:	Gamma
g/l	:	Gram per litre
min	:	Minute
ml	:	Millilitre
mA	:	Milliampere
V	:	Voltage
Å	:	Angstrom
h	:	hour
PVDF	:	Polyvinylidene fluoride
NMP	:	N-Methyl-2-pyrrolidone
mM	:	Millimolar
Mg	:	Magnesium

HRTEM	:	High Resolution Transmission Electron Microscope
XRD	:	X-ray diffraction
XPS	:	X-ray photoelectron spectroscopy
FESEM	:	Field Emission Scanning Electron Microscopy
FTIR	:	Fourier-transform infrared spectroscopy
PL	:	Photoluminescence Spectroscopy
TMDC	:	Raman spectra
MHz	:	Photo Luminiscence
kHz	:	Transition-metal dichalcogenide
w.r.t.	:	Megahertz
nm	:	Kilohertz
μm	:	with respect to
Ag^{-1}	:	Nanometre
^oC	:	Micrometre
Ω	:	Ampere per gram
R_{ct}	:	Degree Celsius
GITT	:	Ohm
EIS	:	Charge transfer resistance
GCD	:	Galvanostatic intermittent titration technique
CV	:	Electrochemical impedence spectroscopy
KOH	:	Galvanostatic charge-discharge
$AlCl_3$	:	Cyclic voltammetry
SHE	:	Potassium hydroxide
Wh	:	Aluminium Chloride
H_xMoO_3	:	Standard Hydrogen Electrode
$mAhg^{-1}$	:	Watt-hour
		Hydrogen doped MoO_3
		Mili Ampere hour per gram